NIMROD simulations of dynamo experiments in cylindrical and spherical geometries

Dalton Schnack,

Ivan Khalzov, Fatima Ebrahimi, Cary Forest,

Introduction

- Two experiments, Madison Plasma Couette Experiment (MPCX) and Madison Plasma Dynamo Experiment (MPDX), have been designed at the University of Wisconsin to study rotating plasma in cylindrical and spherical geometries.
- Experimental novelties:
  - hot, unmagnetized plasma
  - ability to control plasma rotation profile
- Broad class of phenomena can be investigated, such as magnetorotational instability and dynamo.
- These phenomena are important in many astrophysical applications but remain poorly understood.

Goals

- Numerical support of MPCX and MPDX using the extended MHD code, NIMROD:
  - flexibility in geometry and physics
  - realistic experimental conditions
  - importance of “non-MHD” effects (two fluid etc.)
  - optimization of plasma parameters
  - guidance for the experimental operation
- Validation of NIMROD by comparing experimental results with numerical predictions.

Experiments

- Plasma Couette Experiment (MPCX)
- Plasma Dynamo Experiment (MPDX)

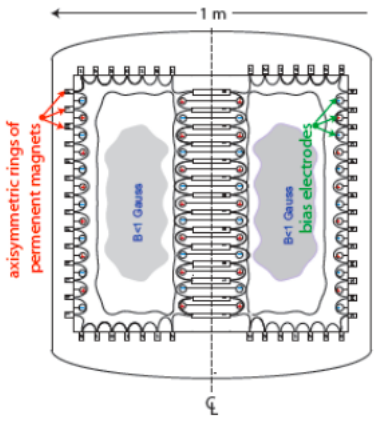

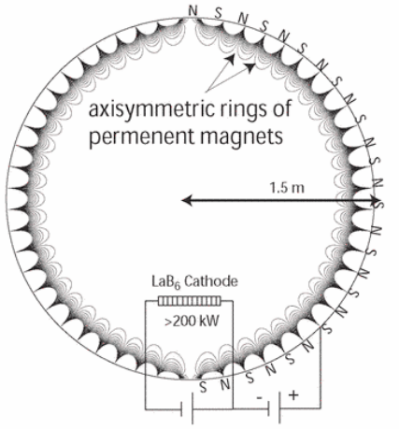

This slide shows sketches of the experiments. MPCX consists of the cylindrical chamber of 1 meter in diameter and 1 meter in height. MPDX is spherical experiment of 3 meter in diameter. Plasma is mostly unmagnetized. The feature of these experiments is the presence of axisymmetric rings of permanent magnets of alternating polarity at the walls of the vessels. The role of these magnets is twofold. First they provide multi-cusp confinement of the plasma.

Novel method of plasma rotation

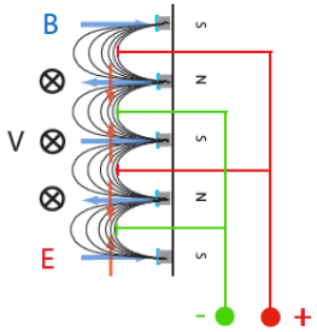

- ExB rotation is induced by applying voltage between magnetic rings
- Velocity profile can be controlled at the boundary by biasing the electrodes with arbitrary potentials
- Typical speed for B=1 T, E=100 V/m

$$V[km/s] = 0.1\frac{E[V/m]}{B[T]} = 10\ km/s$$

And second, by placing electrodes between the rings and applying voltage between the electrodes, it is possible to induce ExB plasma rotation. The novelty of the experiments is the ability to control the rotation profile at the boundary by biasing the electrodes with arbitrary potentials. Typical value of velocity for typical electric and magnetic field is shown on the slide.

Plasma parameters

- Plasma parameters can be varied in wide range:
  -density: $n=10^{17}$-10^{19} m^{-3}
  -ion temperature: T_i=0.5-4 eV
  -electron temperature: T_e=2-25 eV
  -peak speed: V=0-20 km/s
  -ion species: H (1 amu), He (4 amu), Ar (40 amu)
- For hydrogen plasma with V=10 km/s, L=0.5 m, $n=10^{18}$ m^{-3}, T_i=0.5 eV, T_e=25 eV:

$$\text{Magnetic Prandtl}: \quad \mathrm{Pr}=\frac{\nu}{\eta}=0.2\frac{T_e^{3/2}[eV]T_i^{5/2}[eV]}{n[10^{18}m^{-3}]Z\mu_i^2}=4.4$$

$$\text{Reynolds}: \quad \mathrm{Re}=\frac{VL}{\nu}=8\frac{L[m]V[km/s]n[10^{18}m^{-3}]\mu_i^2}{T_i^{5/2}[eV]}=226$$

$$\text{Magnetic Reynolds}: \quad \mathrm{Rm}=\frac{VL}{\eta}=1.6\frac{L[m]V[km/s]T_e^{3/2}[eV]}{Z}=1000$$

$$\text{Mach}: \quad \mathrm{M}=\frac{V}{C_s}=0.1\frac{\mu_i^{1/2}V[km/s]}{T_e^{1/2}[eV]}=0.2$$

$$\text{Hall}: \quad \varepsilon=\frac{c}{L\omega_{pi}}=0.23\frac{\mu_i^{1/2}}{L[m]n^{1/2}[10^{18}m^{-3}]Z}=0.46$$

The use of plasma allows experimentalists to vary parameters in wide range. In our study we introduce several dimensionless numbers. They are magnetic Prandtl Pr (ratio of viscosity to resistivity), Reynolds Re (velocity times size over viscosity), magnetic Reynolds Rm (velocity times size over resistivity), Mach M (velocity over sound speed) and Hall \eps (normalized ion skin depth). For excitation of magnetic dynamo it is important to have relatively high Rm. For typical hydrogen plasma with given parameters Rm can be as high as 1000.

NIMROD – extended MHD code

$$\frac{\partial \mathbf{B}}{\partial t} = -\nabla\times\left(\eta\mathbf{J} - \mathbf{V}\times\mathbf{B} + \frac{1}{ne}\mathbf{J}\times\mathbf{B} - \frac{T}{ne}\nabla n - \frac{1}{ne}\nabla\cdot\Pi_e\right) + \kappa_{divb}\nabla\nabla\cdot\mathbf{B}$$ Faraday's / Ohm's law

$$\mu_0\mathbf{J} = \nabla\times\mathbf{B}$$ low-ω Ampere's law

$$\rho\left(\frac{\partial \mathbf{V}}{\partial t} + \mathbf{V}\cdot\nabla\mathbf{V}\right) = \mathbf{J}\times\mathbf{B} - \nabla p - \nabla\cdot\Pi_i(\mathbf{V})$$ flow evolution

$$\frac{\partial n}{\partial t} + \nabla\cdot(n\mathbf{V}) = \nabla\cdot D\nabla n$$ particle continuity with artificial diffusivity

$$\frac{n}{\gamma - 1}\left(\frac{\partial T_\alpha}{\partial t} + \mathbf{V}_\alpha\cdot\nabla T_\alpha\right) = -p_\alpha\nabla\cdot\mathbf{V}_\alpha - \nabla\cdot\mathbf{q}_\alpha + Q_\alpha$$ temperature evolution

Π_i is a combination of Π_{gv}, $\Pi_{||}$, and $\Pi_\perp$

$$\Pi_{gv} = \frac{m_i p_i}{4eB}\left[\hat{\mathbf{b}}\times\mathbf{W}\cdot\left(\mathbf{I} + 3\hat{\mathbf{b}}\hat{\mathbf{b}}\right) - \left(\mathbf{I} + 3\hat{\mathbf{b}}\hat{\mathbf{b}}\right)\cdot\mathbf{W}\times\hat{\mathbf{b}}\right], \quad \left(\mathbf{W} \equiv \nabla\mathbf{V} + \nabla\mathbf{V}^T - \frac{2}{3}\mathbf{I}\nabla\cdot\mathbf{V}\right)$$

$$\Pi_{||} = \frac{p_i\tau_i}{2}\left(\hat{\mathbf{b}}\cdot\mathbf{W}\cdot\hat{\mathbf{b}}\right)\left(\mathbf{I} - 3\hat{\mathbf{b}}\hat{\mathbf{b}}\right)$$

$$\Pi_\perp \sim -\frac{3p_i m_i^2}{10e^2B^2\tau_i}\mathbf{W}$$ has been treated as $-nm_i\nu_{iso}\,\mathbf{W}$ or $-nm_i\nu_{kin}\,\nabla\mathbf{V}$

$$\mathbf{q}_i = -n\left[\chi_{||i}\hat{\mathbf{b}}\hat{\mathbf{b}} + \chi_{\perp i}\left(\mathbf{I} - \hat{\mathbf{b}}\hat{\mathbf{b}}\right)\right]\cdot\nabla T_i + 2.5p_i(eB)^{-1}\hat{\mathbf{b}}\times\nabla T_i$$

$$\mathbf{q}_e = -n\left[\chi_{||e}\hat{\mathbf{b}}\hat{\mathbf{b}} + \chi_{\perp e}\left(\mathbf{I} - \hat{\mathbf{b}}\hat{\mathbf{b}}\right)\right]\cdot\nabla T_e - 2.5p_e(eB)^{-1}\hat{\mathbf{b}}\times\nabla T_e$$

NIMROD is based on fluid-like description of plasma. The full system, which can be solved by NIMROD is shown on the slide. In NIMROD it is possible to study plasma beyond the simple one-fluid MHD model: one can include into consideration two-fluid effects, gyro-viscosity, effects due to parallel and perpendicular thermal conductivities etc.

Isothermal model (non-dimensional form)

$$\dot{n} + \nabla\cdot(n\mathbf{v}) = 0$$

$$n\dot{\mathbf{v}} + n(\mathbf{v}\cdot\nabla)\mathbf{v} + \frac{1}{\mathrm{M}^2}\nabla n = (\nabla\times\mathbf{b})\times\mathbf{b} + \frac{1}{\mathrm{Re}}\nabla\cdot\Pi$$

$$\dot{\mathbf{b}} = \nabla\times\left(\mathbf{v}\times\mathbf{b} - \frac{\varepsilon}{n}(\nabla\times\mathbf{b})\times\mathbf{b}\right) + \frac{1}{\mathrm{Rm}}\nabla^2\mathbf{b}$$

$$\Pi_{ij} = \partial_i v_j + \partial_j v_i - \frac{2}{3}\delta_{ij}\partial_m v_m$$

where $n = \frac{\rho}{\rho_0}$, $\mathbf{v} = \frac{\mathbf{V}}{V}$, $\mathbf{b} = \frac{\mathbf{B}}{V\sqrt{4\pi\rho_0}}$

- Boundary conditions:
  - No-slip for velocity
  - Perfectly conducting for magnetic field

In our study we use isothermal model, which in non-dimensional form is shown on the slide. Here M is Mach number (ratio of typical velocity to sound speed), Re is hydrodynamic Reynolds number, Rm is magnetic Reynolds number. We also include two fluid effects into consideration, they are characterized by Hall parameter \epsilon (normalized ion skin depth). In this model density is normalized by averaged density \rho_0, velocity by the peak velocity of flow V, normalized magnetic field b is the ratio of local Alfven velocity to the peak velocity. For boundary conditions we assume no-slip conditions for velocity and perfectly conducting for magnetic field.

Drive with multi-cusp magnetic field

- NIMROD boundary conditions are modified to include effects of multi-cusp magnetic field and applied tangential electric field
- Different types of flows (rigid, Von Karman etc.) are simulated successfully in both geometries

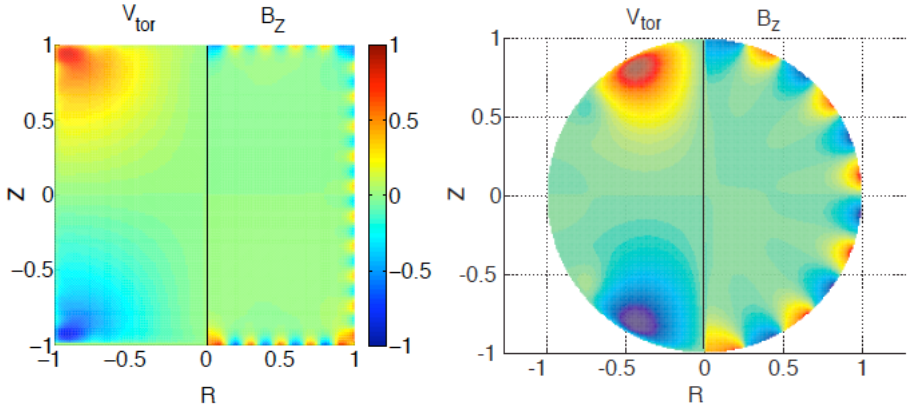

To simulate the applied poloidal multi-cusp magnetic field and the tangential electric field we modified NIMROD equilibrium and boundary conditions. The boundary electric field can be modulated appropriately to obtain different flows. Several types of flows are simulated successfully in both geometries. The figures show the results for Von Karman flow – flow with counter-rotating top and bottom end caps (for cylinder) and top and bottom hemispheres (for sphere). Left part of each figure is a structure of toroidal flow and right part is the structure of z-component of multi-cusp magnetic field

Von Karman flow in cylinder: equilibrium

- In our study we assume:
  - no cusp field, no applied electric field
  - perfectly conducting, no-slip boundaries
  - plasma is driven by walls rotating differentially with angular velocity, corresponding to Von Karman flow

    top (0<r<1, z=1): Ω=1

    side (r=1, -1<z<1): Ω=z

    bottom (0<r<1, z=-1) Ω=-1

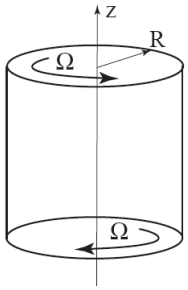

- Axisymmetric flow and density for Re=200, M=1

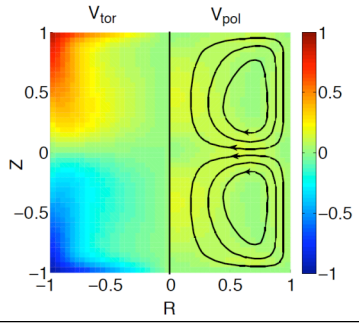

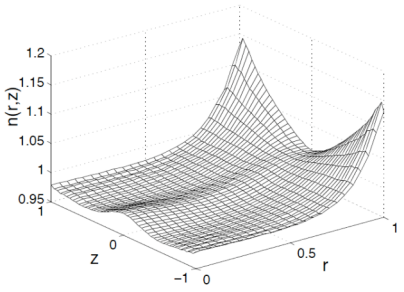

For simplicity, in the rest of our study we assume that there are no cusp magnetic field, no applied electric field and the flow is driven by differentially rotating walls (as in Taylor-Couette flow). In cylindrical case the dependence of the angular velocity of the walls is the following: top and bottom disks are rotating with the same angular velocity but in opposite directions and the side wall has linear dependence of angular velocity on z to match the rotation of top and bottom disks. This is the so-called Von Karman flow. Left figure shows the structure of axisymmetric Von Karman flow in cylinder (toroiadal rotation and poloidal circulation), right figure shows the structure of density for the case with Reynolds=200, Mach=1

Von Karman flow in cylinder: stability

- Axisymmetric Von Karman flow is hydrodynamically unstable when Re>170 (Kelvin-Helmholtz instability)
- The instability saturates at new stable non-axisymmetric equilibrium, which consists of even azimuthal harmonics with m=0, 2, 4 etc.
- Such transition to non-axisymmetric equilibrium is crucial for dynamo

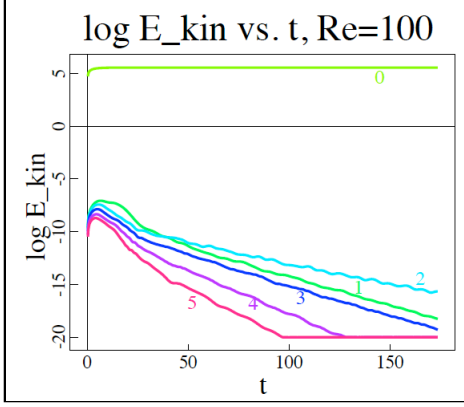

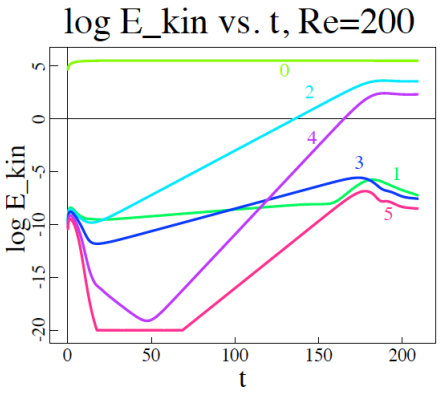

Such Von Karman flow becomes hydrodynamically unstable when Re>170. This is illustrated by figures: for Re=100 kinetic energy of non-axisymmetric perturbations is decreasing, for Re=200 energy of perturbations is growing exponentially. Instability saturates at new non-axisymmetric equilibrium, which consists of even azimuthal harmonics with m=0, 2, 4… . Such transition to non-axisymmetric equilibrium is crucial for dynamo

Kinematic dynamo in cylinder

- Find velocity $\mathbf{v}_0$ as a solution to Navier-Stokes equation for some Re
- Solve eigenvalue problem for magnetic field **b** with different Rm

$$\gamma \mathbf{b} = \nabla \times \left(\mathbf{v}_0 \times \mathbf{b} \right) + \frac{1}{\mathrm{Rm}} \nabla^2 \mathbf{b}$$

- Find the growth rate, determine the critical Rm

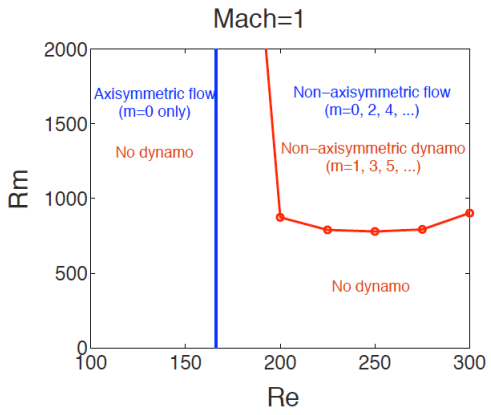

First step in study of dynamo is solving the kinematic dynamo problem: determining the possibility of excitation of magnetic field for a given flow structure. For a fixed Reynolds number we solve Navier-Stokes equation and find velocity structure. Using that velocity, we solve induction equation as an eigenvalue problem for magnetic field with different magnetic Reynolds numbers. As a result we determine the critical magnetic Reynolds above which the dynamo excitation is possible. The figure shows the dependence of the critical Rm on Re for Mach=1 (red curve). The blue line separates the regions of axisymmetric (Re<170) and non-axisymmetric (Re>170) flows. As our results show, the kinematic dynamo is not possible in axisymmetric flow. In non-axisymmetric flow the dynamo appears as a growing magnetic field with odd azimuthal harmonics (m=1,3,5..).

Kinematic dynamo in cylinder: compressibility

- Dynamo effect depends on compressibility:

$$\dot{\mathbf{b}} = (\mathbf{b}\cdot\nabla)\mathbf{v} - (\mathbf{v}\cdot\nabla)\mathbf{b} - (\nabla\cdot\mathbf{v})\mathbf{b} + \frac{1}{\mathrm{Rm}}\nabla^2\mathbf{b}$$

- Compressibility is related to Mach number $M=V/C_s$

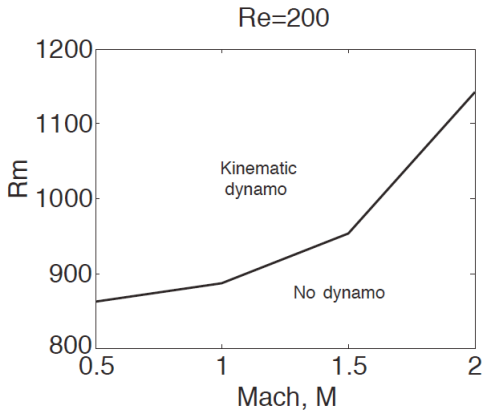

This slide shows the effect of compressibility on the kinematic dynamo. Growth rate of magnetic field in induction equation depends on compressibility (equation). Compressibility is related to Mach number (ratio of peak velocity to sound speed): the higher Mach the more compressible fluid. Figure shows the dependence of critical magnetic Reynolds on Mach.

Dynamo in cylinder: MHD saturation

- Re=200, Rm=1000, M=1 (μ_i=1, n=10^{20} m^{-3}, T_e=11 eV, T_i=5.4 eV, V=33 km/s)

Kinetic energy vs. time

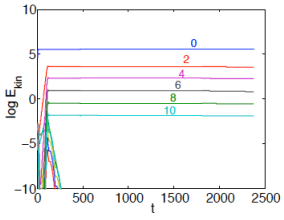

Magnetic energy vs. time

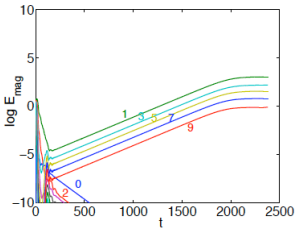

Iso-surfaces $|V_{alfven}|/V$=0.02
(|B|=3 Gauss)

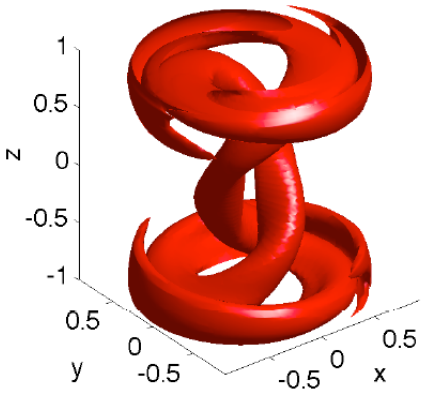

This slide shows the stage of saturation of magnetic dynamo in one fluid MHD model for non-dimensional parameters Reynolds=200, magnetic Reynolds=1000, Mach=1 (the corresponding physical parameters are shown in brackets). Left side is the time evolution of logarithm of kinetic and magnetic energies of different azimuthal harmonics. At t~100 flow becomes steady and non-axisymmetric with even harmonics (m=0,2,4,…). In such flow the dynamo is excited: magnetic field of odd harmonics (m=1,3,5,…) grows exponentially in time till saturation at t~2000. The saturated magnetic field has about 1% of energy of the flow. The structure of the saturated magnetic field is shown on the right. This is iso-surface (surface of the same value) of magnetic field amplitude, corresponding to ratio of Alfven speed to peak flow speed of 0.02 (for listed physical parameters it is about 3 Gauss). One can see the dominated m=1 structure of the dynamo.

Dynamo in cylinder: Hall effect

- Re=200, Rm=1000, M=1, ε=0.05 (μ_i=1, n=10^{20} m^{-3}, T_e=11 eV, T_i=5.4 eV, V=33 km/s)

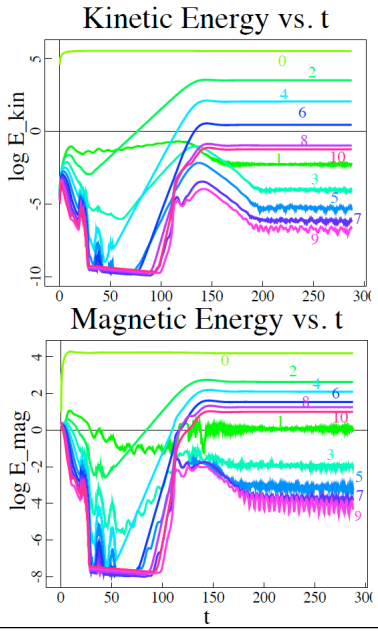

Iso-surfaces of magnetic field, $|V_{alfven}|/V=0.02$ ($|B|$=3 Gauss)

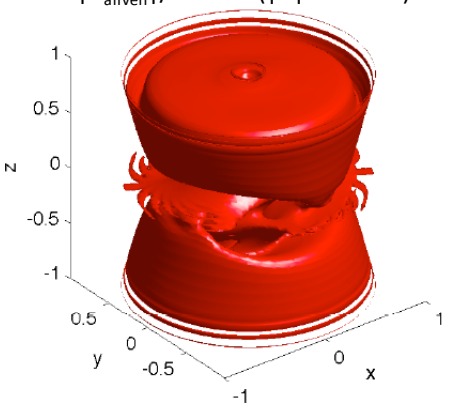

- Hall effect changes saturation completely as compared to MHD dynamo
- Saturated magnetic field has mainly azimuthal component B_ϕ with m=0

The growth and saturation of magnetic field in Hall MHD model is shown on this slide. We use the same parameters as in MHD case, but turn the Hall term on. The effect is pronounced: magnetic field saturates at a new state with even harmonics (m=0,2,4,..) – see the bottom left figure. Such difference between MHD and Hall MHD dynamos is (most likely) due to the break of the symmetry in Hall MHD system. The Hall MHD equations change if the sign of magnetic field is changed (i.e, if B becomes –B); the MHD equations don't.

Dynamo in cylinder: Hall effect

- Hall dynamo exists in the regime with no kinematic dynamo!
- Subcritical excitation?

Re=100, Rm=1000, M=1, ε=0.05

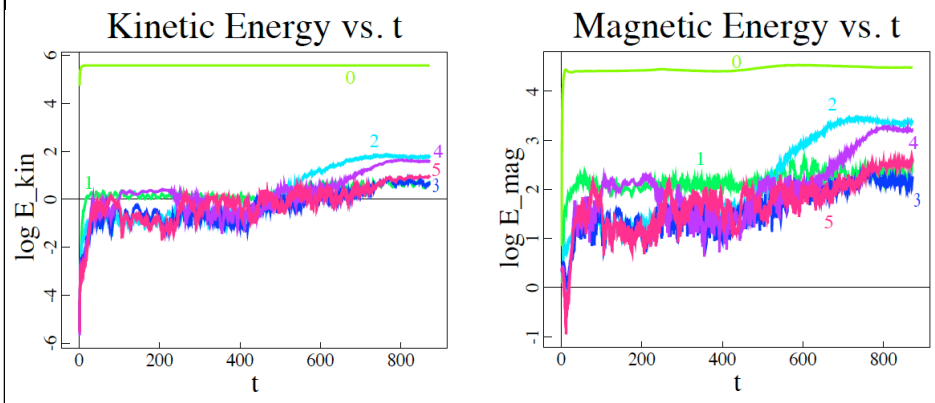

The interesting point about Hall MHD dynamo is that it can be excited in the regime, where there is no kinematic dynamo (non-kinematic regime). Such case with Re=100, Rm=1000, Mach=1 and Hall=0.05 is shown on figures. This might mean that the Hall dynamo is subcritical (non-linear), i.e., it can be excited in non-kinematic regime if the amplitude of the initial perturbation is large enough. However these question should be studied more carefully.

Von Karman flow in sphere: equilibrium

- We assume:
  - perfectly conducting, no-slip boundaries
  - plasma is driven by walls rotating differentially with velocity:
    $v_{tor}=\sin 2\Theta$, $-\pi/2<\Theta<\pi/2$
- Axisymmetric flow and density for Re=150, M=0.2

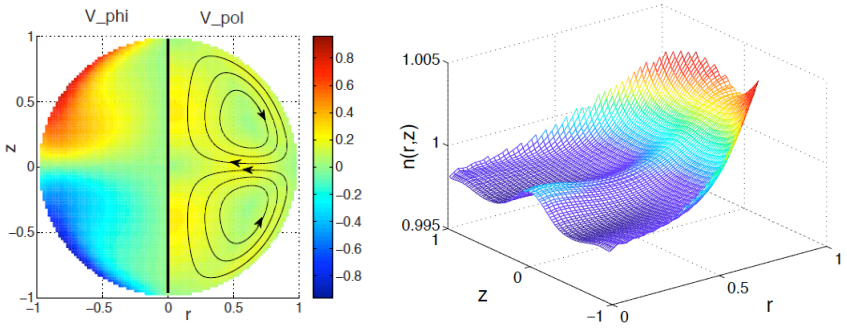

Analogous study has been performed for spherical geometry. For sphere we also assume the differential rotation of the walls of the form (equation), which corresponds counter-rotating hemispheres with angular velocity changing linearly with height. The figures show the structure of the flow (toroidal rotation and poloidal circulation) and the density for Re=150 and Mach=0.2

Von Karman flow in sphere: stability

- Similar to cylinder, axisymmetric Von Karman flow in sphere is hydrodynamically unstable when Re>120
- The instability saturates at new stable non-axisymmetric equilibrium, which consists of even azimuthal harmonics with m=0, 2, 4 etc.

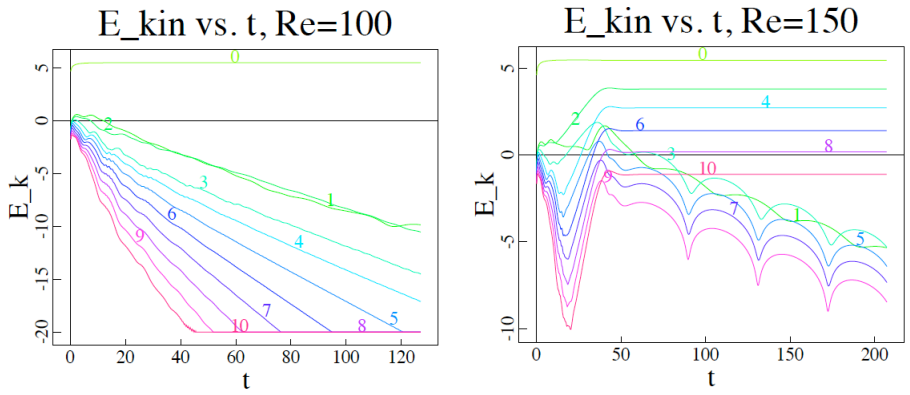

Similar to cylinder, axisymmetric Von Karman flow in sphere is hydrodynamically unstable when Re>120. The instability saturates at new stable non-axisymmetric equilibrium, which consists of even azimuthal harmonics with m=0, 2, 4 etc. As in cylindrical case, such transition to a new equilibrium makes possible the excitation of the kinematic dynamo.

Dynamo in sphere: Re=150, Rm=2000, M=0.2
(μ_i=1, n=10^{18} m^{-3}, T_e=20.5 eV, T_i=0.9 eV, V=9 km/s)

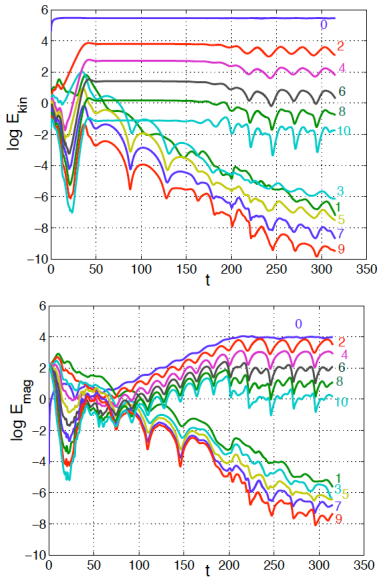

Iso-surfaces of magnetic field at t=309.16,
$|V_{alfven}|/V$=0.12 ($|B|$=0.5 Gauss)

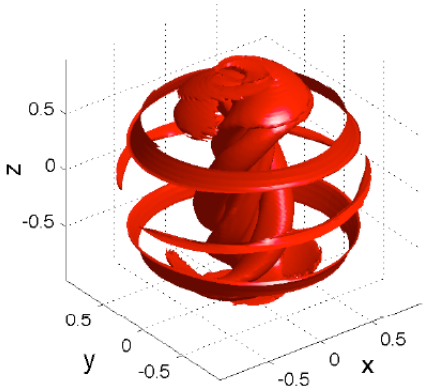

This slide shows an example of spherical dynamo for Re=150, Rm=2000, M=0.2 (corresponding physical parameters are shown in brackets). Figures on left are the time evolution of logarithm of kinetic and magnetic energies of different azimuthal harmonics. At t~50 flow becomes steady and non-axisymmetric with even harmonics (m=0,2,4,…). In such flow the dynamo is excited: magnetic field of even harmonics (m=0,2,4,…) grows exponentially in time till saturation at t~200. The saturated magnetic filed and flow are oscillating. The structure of the saturated magnetic field is shown on the right for t=309. This is iso-surfaces of magnetic field amplitude, corresponding to ratio of Alfven speed to peak flow speed of 0.12 (for listed physical parameters it is about 3 Gauss).

Dynamo in sphere: domain of parameters

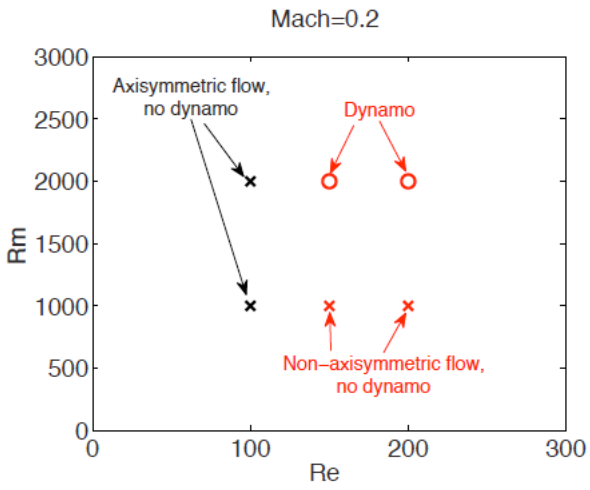

The possibility of MHD dynamo in sphere has been checked for different parameters. On Rm-Re plain the domain of dynamo parameters is on the right from Re~120 and above Rm~1500, which is in qualitative agreement with cylindrical results.

Conclusions

- NIMROD simulations can provide a strong numerical support for MPCX and MPDX
- Our results show that magnetic field can be generated in both cylindrical and spherical geometries for realistic experimental conditions
- Effect of compressibility and two-fluid (Hall) effects on dynamo have been studied:

  - the more compressible the fluid the higher critical Rm

  - Hall effect changes the saturation of the dynamo field

  - there is a possibility of subcritical dynamo excitation in Hall MHD (this question is under consideration)